CrossMark

Electrodeposition and Properties of Composites Consisting of Carbon Nanotubes and Copper

Shaoli Fu, Xiaohong Chen, Ping Liu, Wei Liu, Pengzhong Liu, Ke Zhang, and Haohan Chen

Copper–matrix–carbon nanotubes (Cu–CNTs) composite films were prepared in a Cu plating solution with multiwall carbon nanotubes (MWCNTs) using electrodeposition. The MWCNTs surface treatment method, electroplating solution system, electroplating conditions, heat treatment process and other parameters of this process are discussed. The results showed that MWCNTs purified by HCl treatment and dispersed by stearyltrimethylammonium bromide are more suitable as add-on materials for the preparation of the copper matrix composite films by electrodeposition. An appropriate heat treatment process was able to improve the structures and properties of the composite films. The final products showed that the MWCNTs were evenly distributed in the composite films and joined with the copper grains to form a mutually entangled mesh structure with excellent corrosion resistance ($3.19 \times 10^{-8} \, \Omega \, M$) and a hardness of 53.5 HV. All this was possible through extensive optimization of the electrodeposition and post-treatment parameters.

1. Introduction

Copper and its alloys are required to have both high strength and high electric and thermal conductivity to be used in electrical and electronic applications (Ref 1, 2). Pure copper indeed shows these characteristics but has low strength. Therefore, the development of the copper matrix composites with good electrical and thermal conductivity as well as high strength is very important.

Since their discovery in 1991 (Ref 3-6), carbon nanotubes (CNTs) have been actively studied because of their excellent mechanical, electrical and thermal properties (Ref 7-9) as well as fillers for different composites. In particular, combination of the metals with CNTs showed significant improvements in the performance of the metal matrices (Ref 10-15).

There are various methodologies for fabricating metal–CNTs composite films, such as powder metallurgy (Ref 16), electroless deposition (Ref 17), electrophoresis deposition (Ref 18), electrodeposition (Ref 19, 20). The latter one proved to be an effective way for obtaining metal/carbon composites with excellent interfacial bonding. The extraordinary strength of these composites is attributed to the metal grain refinement and homogeneous dispersion of carbon nanomaterials (Ref 21). Thus, one can conclude that a homogeneous dispersion and co-deposition of metals and CNTs are very important to form a homogeneous dispersion of CNTs in the composite films (Ref 22, 23).

Shaoli Fu, Xiaohong Chen, Ping Liu, Wei Liu, Pengzhong Liu, Ke Zhang, and **Haohan Chen**, School of Materials Science and Engineering, University of Shanghai for Science and Technology, Shanghai 200093, China. Contact e-mails: 1643691446@qq.com, lpz0328@163.com, lusst008@163.com.

In this paper, we discuss electrodeposition-based fabrication method of a composite consisting of Cu matrix and multiwall carbon nanotubes (MWCNTs). We optimized fabrication parameters based on the analysis of the structure and the performance of the composite with the goal to obtain a composite film with the best combination of electrical conductivity, mechanical properties and corrosion resistance.

2. Experimental

2.1 Materials and Equipment

The MWCNTs, prepared by the chemical vapor deposition (CVD), with diameters 20-30 nm, lengths 10-30 μm, 95% purity and 2.1 g/cm^3 density were provided by Chengdu Organic Chemicals Co., Ltd. Chemicals used in our experiments [such as HCl, H_2SO_4, $CuSO_4$, $NaCH_3COO$, Na_2SO_4, NaOH, ethanol, acetone, NaCl and stearyltrimethylammonium bromide (STAB)] were purchased from Shanghai Sinopharm Chemical Reagent Co., Ltd. All of them were at least analytically pure. Φ5 samples, platinum and saturated calomel electrode (SCE) acted as working, counter and reference electrodes, respectively.

2.2 Surface Modification of MWCNTs

The surface modification on MWCNTs had a twofold purpose. First one was to purify the surface of MWCNTs from impurities such as metal catalyst particles, amorphous carbon and graphite pieces, all of which were removed by HCl. Second, the surface was modified to introduce defects to the MWCNTs surface. These defects act like anchors to the active groups of the surfactants (such as STAB), which improve the surface potential of MWCNTs and ensure smooth electronic transmission and uniform dispersion of MWCNTs. In order to achieve the above effect, we used the following methodology.

First, 2.5 g of MWCNTs were added to 250 mL of acetone and ultrasonicated for 1 h to remove the organic impurities and

amorphous carbon, and further they were filtrated and cleaned with the deionized water. Purified MWCNTs were then put into 250 mL of 5 mol/L HCl solution, stirred for 12 h, and then washed by deionized water till the filtrate had neutral pH. Filtered MWCNTs were then heated at 80 °C for 24 h, ground into powders, and put back again into the drying oven. Next, MWCNTs were placed in 200 mL of deionized water containing different amounts of STAB and stirred for 6 h. After that, MWCNTs were allowed to stay in the solution for 24 h without any additional agitation. The Zeta potential was determined before and after the treatment, which was used to judge the effectiveness of the surface treatment and to optimize its parameters.

2.3 Determination of Preparation Process

Copper foil (25 × 20 mm) and platinum-plate electrode (30 × 30 mm) were used as cathode and anode, respectively. The Cu-MWCNTs composite films were prepared by pulse-reverse current deposition. The starting concentrations of $CuSO_4$, H_2SO_4, STAB, HCl and MWCNTs were 50, 50, 0.5, 0.006 and 2 g/L, respectively. We changed these concentrations throughout the experiments together with some other process parameters to achieve the best plating results. A successful plating was judged by the surface morphology and conductivity of Cu–MWCNTs composite films.

2.4 Characterization of the Composite Films

Field emission scanning electron microscope (FESEM, Quanta FEG 450, FEI, USA), laser Raman spectrometer (Raman Station 400F with 514 nm excitation wavelength, PerkinElmer, USA), Thermogravimetric analyzer (TGA, Pyris 1, PerkinElmer, USA), four-probe resistance test analyzer (Keithley 4200, Tektronix/Keithley, USA), microhardness tester (HXD-1000 TMC/LCD, Shanghai Taiming Optical Instruments Co., Ltd, China) and electrochemical workstation (CHI 1140C, Shanghai Chenhua Instruments Co., Ltd, China) were used to study the surface morphology, electrical conductivity, hardness and corrosion resistance of the Cu–MWCNTs composite films, respectively.

3. Results and Discussion

3.1 Surface Modification of MWCNTs

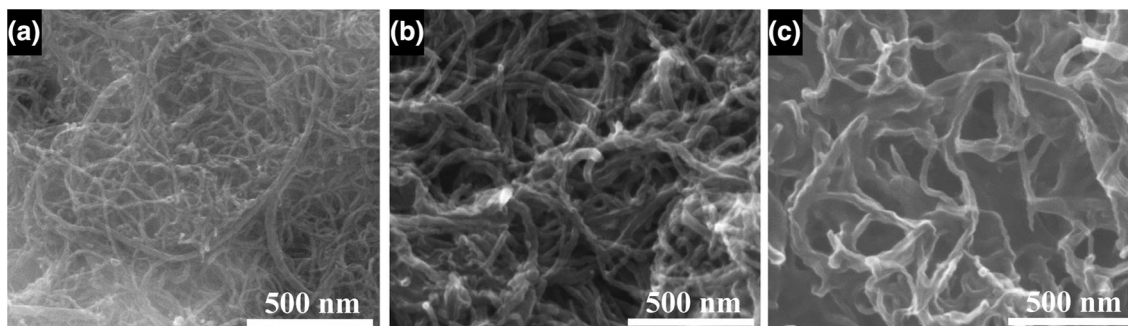Comparing with the untreated MWCNTs (shown in Fig. 1a), MWCNTs purified by HCl (see Fig. 1b) had a relatively clean surface and hardly any residual impurities. Raman spectra of MWCNTs before and after HCl treatment (see Fig. 2) showed typical MWCNTs peaks: D, G^- and G^+ (Ref 24, 25). After the HCl purification, the value of $R = I_D/I_G$ decreased from 1.57 to 1.19, indicating that the disorder degree decreased, while the degree of relative graphitization of MWCNTs improved.

Prior to the dispersion, MWCNTs were agglomerated (see Fig. 1b), but after the treatment with STAB, they became uniformly distributed (see Fig. 1c). Treatment with STAB also affected the surface potential of MWCNTs: When the concentration of STAB increased from 0 to 0.5 g/L, the surface potential of MWCNTs also increased from − 27.15 to 58.25 mV (see Fig. 3). However, with further increase in STAB concentration from 0.5 to 0.7 g/L, the MWCNTs surface potential plateaued or even slightly decreased (see Fig. 3).

TGA was used to characterize the surface modification of MWCNTs (see Fig. 4). The samples were heated at 10 °C/min up to 700 °C under a nitrogen flow. A slight weight loss before 300 °C could be observed in two curves for both samples, which can be assigned to the absorbed moisture release. The weight loss of MWCNTs was small from 300 to 500 °C, and it was only 3.3% till 700 °C. But the weight of surface-modified MWCNTs decreased rapidly between 300 and 500 °C and then plateaued. The overall weight loss of modified MWCNTs was ∼ 26%. Such strong weight loss indicates that STAB was
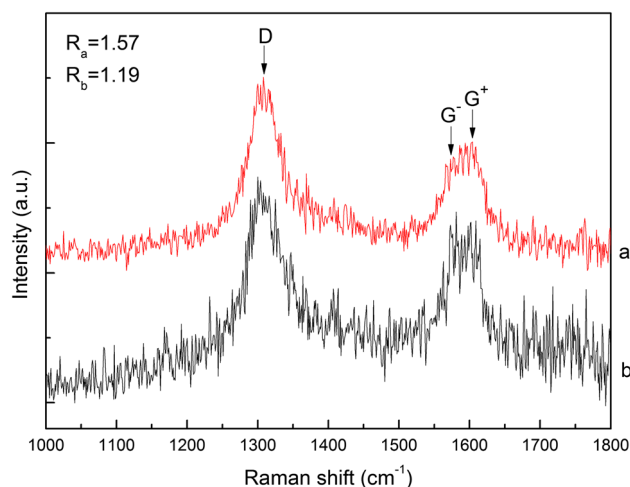

Fig. 2 Raman spectra of MWCNTs before (a) and after (b) HCl treatment

Fig. 1 Morphologies of multiwall carbon nanotubes (MWCNTs) (a) before and (b) after HCl treatment, and (c) after stearyltrimethylammonium bromide (STAB) dispersion treatment

indeed coated on the surface of MWCNTs. It laid the foundation of the subsequent process.

3.2 Effect of the Electroplating Solution Parameters

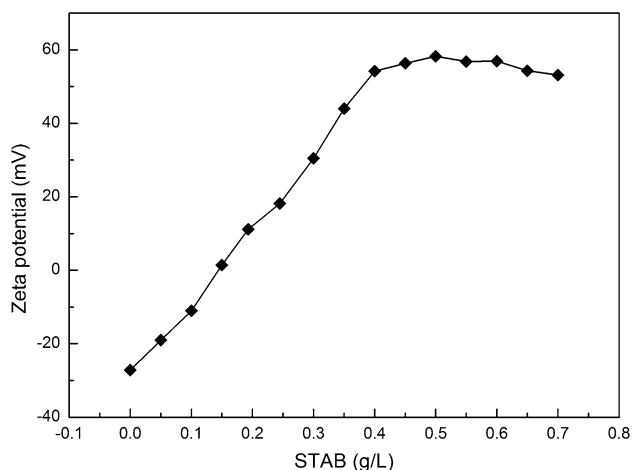MWCNTs can adsorb metal or hydrogen ions from the electroplating solution, then become positively charged (Ref

Fig. 3 Relationship between STAB concentration used for MWCNT treatment and MWCNT surface potential
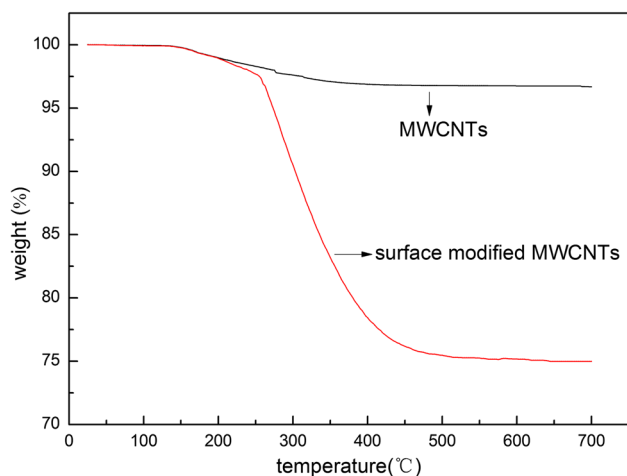

Fig. 4 The TGA data of pristine MWCNTs and surface-modified MWCNTs

26) and move to the cathode. Thus, ion concentrations in the electroplating solutions need thorough optimization. At pH = 2, MWCNTs distributed evenly in the composite films and formed interconnected networks (see Fig. 5b). Very high or very low pH had adverse effects on the composite thin films and influenced their electrical properties (Fig. 6). For example, when the pH value decreased to 1 (Fig. 5a), the copper grains in composite films dominated, which might be due to the hydrogen evolution at increased H^+ concentration and impeded MWCNTs adsorption at the cathode surface. When the pH value increased to 3 or 4 (Fig. 5c and d), the MWCNTs content in composite films gradually decreased and MWCNTs were no longer closely intertwined. The reason for this phenomenon is decrease in H^+ in electroplating solution, which reduces competitive adsorption against copper ions. When MWCNTs easily absorb copper ions, it affects their adsorption and deposition on the cathode.

When the concentration of MWCNTs in the electroplating solution was 1 g/L (Fig. 7a), only some MWCNTs were found in the composite films. The MWCNTs did not bond to each other, and copper grains were in the adhered state. When the MWCNTs concentration was increased to 3 g/L (Fig. 7b), they became better distributed among the copper grains, interconnected with each other, and attached to the copper matrix. There was hardly any adhesion between the copper grains because their growth was hindered by the adsorbed MWCNTs on their surface. The absorption of MWCNTs could also reduce the surface energy required for nucleation of copper grains; thus, more copper particles nucleated simultaneously reducing
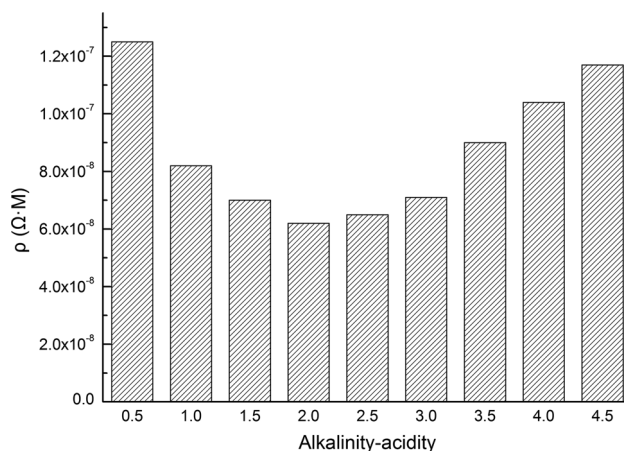

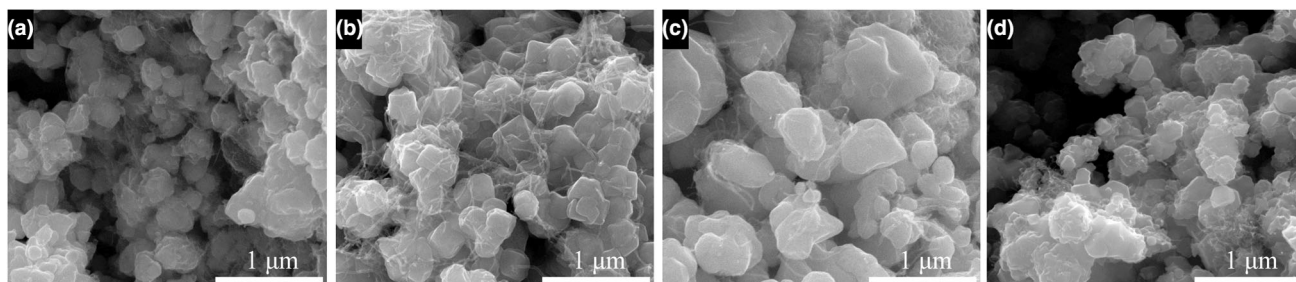**Fig. 6** Electrical conductivity of composite films as function of the pH during electroplating

Fig. 5 Effect of the electroplating solution pH on composite films morphology: (a) pH = 1; (b) pH = 2; (c) pH = 3; (d) pH = 4
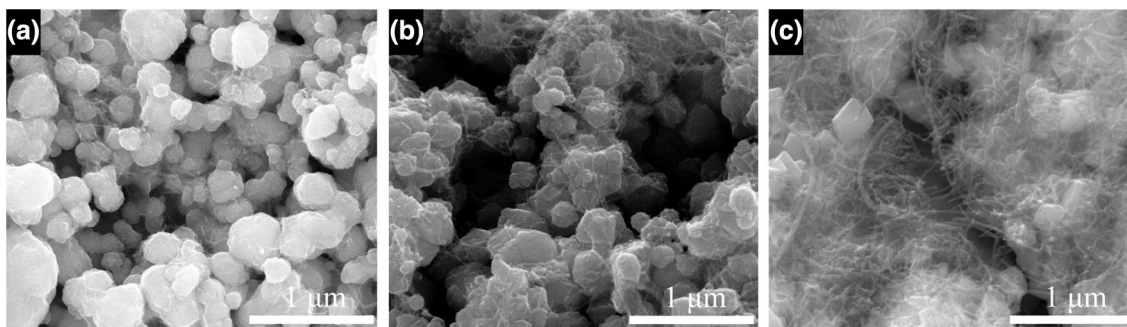
Fig. 7 Effects of different MCNT concentrations in electroplating solution on composite film morphology: (a) 1 g/L; (b) 3 g/L; (c) 5 g/L
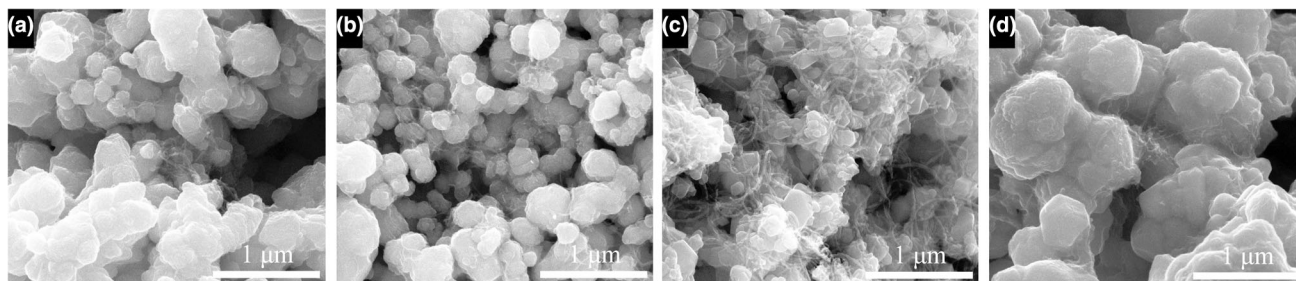

Fig. 8 Composite film morphology at different current densities: (a) 5 A/dm^2; (b) 10 A/dm^2; (c) 20 A/dm^2; (d) 30 A/dm^2

overall grain size. When the concentration of MWCNTs in electroplating solution was further increased to 5 g/L (Fig. 7c), intertwined, segregated and agglomerated MWCNTs deposited in the composite films, but only some copper grains were coated by MWCNTs.

3.3 Effect of Electroplating Conditions on the Composite Films

We used the pulse-reverse electrodeposition process with equal positive (T_{pos}) and negative (T_{neg}) currents and densities. Pulse current density had opposite effect on MWCNTs deposition rate. At low current density, the increase in current density would elevate cathode overpotential as well as the electric field force on metal ions and nanoparticles resulting in more pronounced shapes of the grains (Fig. 8a and b). As copper ions reduced to metallic copper, the MWCNTs were adsorbed and deposited at the cathode (Ref 27). When the current density reached to 20 A/dm^2 (Fig. 8c), no large copper grains were observed in the composite films. At the same time, the MWCNTs were evenly distributed and formed intertwined networks with copper grains. On the other hand, when the current density was further increased (Fig. 8d), the metal deposition became rapid, while the migration velocity of MWCNTs to the cathode did not significantly increase, resulting in larger Cu particle sizes and less MWCNTs intertwined with copper grains.

3.4 Effect of Heat Treatment

After annealing, adhesion between copper and MWCNTs became better (see Fig. 9a) and the electrical resistivity of composite films significantly decreased (Fig. 10), which was caused by the desorption of the gas and the STAB at the contact sites of copper and MWCNTs (Ref 28). After the annealing treatment at 300 °C (Fig. 9b), the surface of composite films became smooth. After the annealing treatment at 400 °C (Fig. 9c), the surface of composite films became even smoother with more uniform copper grains and the lowest electrical resistivity was achieved as well. With the annealing temperature of 500 °C (Fig. 9d), the electrical resistivity of composite films increased due to the formation of recrystallized small copper grains (Ref 29), which increased the scattering of surface electrons (Ref 30).

3.5 Performance Characterization

Concentration of MWCNTs in the Cu–MWCNTs films was calculated by the following equation:

$$\eta = \frac{m_1 - m_2}{M_2 - M_1} \times 100\%, \qquad \text{(Eq 1)}$$

where m_1 is the additional amount of MWCNTs, m_2 is the residual amount of MWCNTs in electroplating solution, M_1 is the weight of the cathode substrate and M_2 is the total mass of the cathode substrate and composite films. Concentration of MWCNTs in the composite films for the best electroplating conditions should be 0.75 wt.%.

SEM analysis (shown in Fig. 11) revealed a 20-μm-thick smooth Cu–CNTs composite films without any significant defects. We believe that smooth films like this are obtained when the composite electrodeposition finishes at the same time as the dissolution.

Raman spectra of the Cu–CNTs composite films showed MWCNTs' characteristic peaks, confirming MWCNTs presence in the copper matrix (see Fig. 12) (Ref 31). Their R value is 1.12, which is slightly lower than the value of 1.19 before deposition. We believe annealing-induced STAB desorption helped MWCNTs avoid damage during electrodeposition, and thus, they have less disorder and defects.
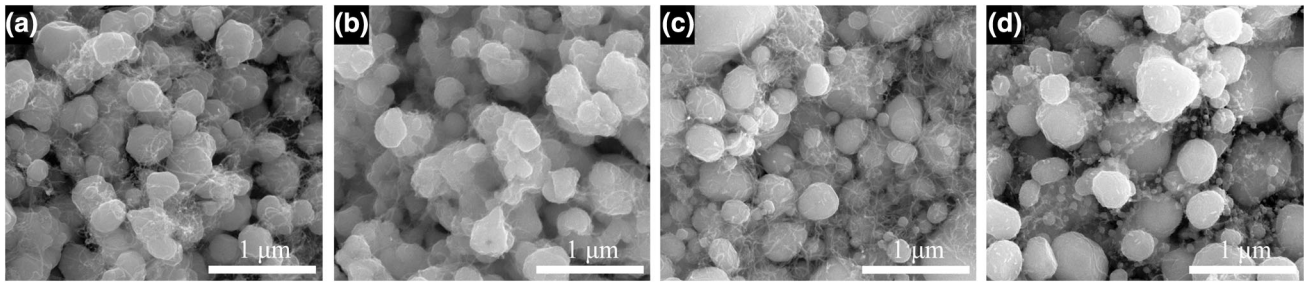
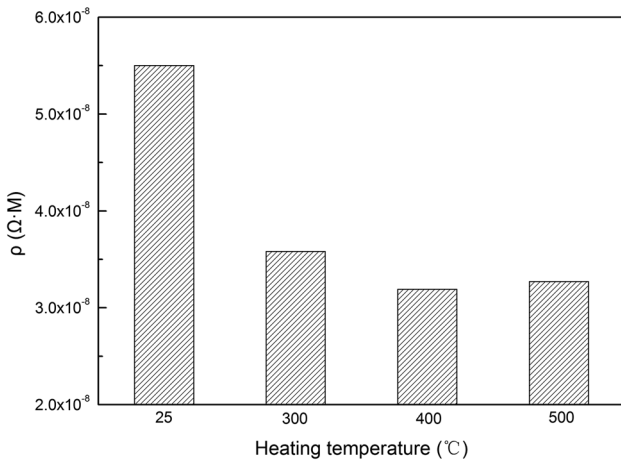**Fig. 9** Composite film morphology after annealing at (a) 25 °C, (b) 300 °C, (c) 400 °C and (d) 500 °C

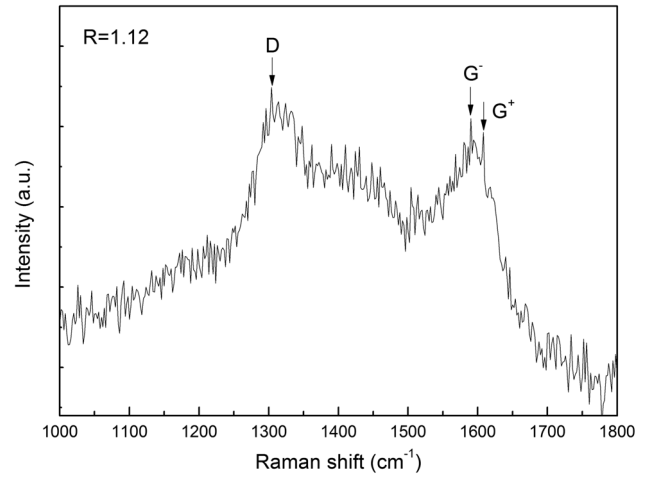**Fig. 10** Electrical conductivity of composite films as function of annealing temperature

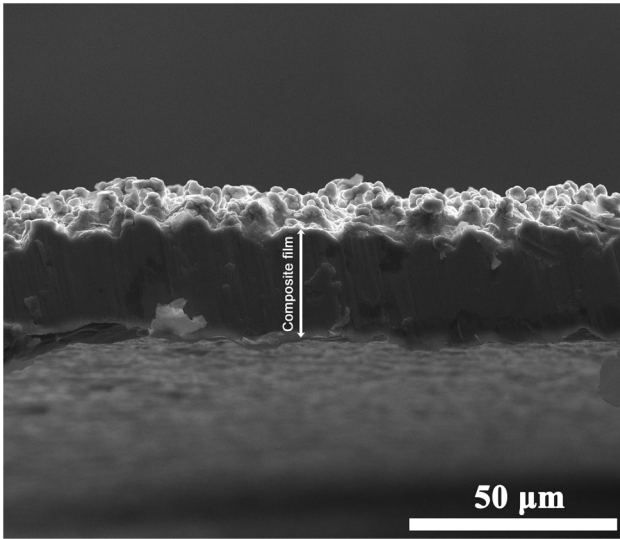

Fig. 12 Raman spectra of the composite films

Fig. 11 Cross-sectional SEM image of Cu-MWCNTs composite films

Fig. 13 Tafel plots of copper and composite films in 0.1 M NaCl solution

Figure 13 shows Tafel plots of copper and Cu–MWCNTs composite films in 0.1 M NaCl. The corrosion potential (V_{corr}) of the Cu–MWCNTs composite films is shifted positively, and the corrosion current (I_{corr}) is significantly lower than that of copper films. The corrosion inhibition efficiency (η) of the Cu–MWCNTs composite was calculated to be 70% by using the following equation:

$$\eta = \frac{I_{corr(copper\ film)} - I_{corr(Cu-MWCNT\ composite)}}{I_{corr(copper\ film)}} \times 100\%. \quad (Eq\ 2)$$

According to Faraday's law, corrosion rate (CR) can be calculated as follows:

Table 1 Test results of copper and composite films

Material	E_{corr}, V/cm^2	I_{corr}, A/cm^2	CR, mm/year	η, %	Resistivity ρ, $\Omega \cdot$M	Vickers hardness, HV
Composite film	-0.32	0.003	34.67	70%	3.19×10^{-8}	53.5
Copper film	-0.57	0.010	115.56	…	3.68×10^{-8}	43.5

$$CR = K \cdot \frac{I_{corr}}{\rho} \cdot EW, \qquad (Eq\ 3)$$

where K is the corrosion rate constant equal to 3.27×10^{-3} mm g/(μ A cm year), ρ is the density of copper equal to 8.97 g/cm^3 and EW is an equivalent weight, calculated by Eq 4:

$$EW = \frac{W}{n}, \qquad (Eq\ 4)$$

where W is the atomic weight of the element (equal to 63.5 for Cu) and n is the number of electrons required by atomic oxidation during the corrosion process (equal to 2 for copper). EW for Cu is equal to 31.7.

The calculated results are shown in Table 1. We can see that the Cu–MWCNTs composite films had better corrosion resistance compared to pure Cu films which is attributed to the MWCNTs embedded in copper grains and grain boundaries. And the MWCNTs could not only refine copper grains and enhance their density, but also hinder the erosion of the internal coating by corrosive liquid.

Electrical conductivity and Vickers hardness of the composite films improved significantly compared to the pure copper films (see Table 1): The resistivity decreased by $\sim 13\%$, while the Vickers hardness increased by $\sim 23\%$. Such improvements are caused by a three-dimensional interconnected conductive mesh structure that MWCNTs formed in the films. This structure reinforces the matrix as well as allows electrons to travel not only through the Cu–Cu transport channels, but also through the MWCNTs–MWCNTs and Cu–MWCNTs ones.

4. Conclusions

Cu–MWCNTs composite films were prepared by electrodeposition. The best composite films were obtained when: (1) MWCNTs were purified by HCl; (2) the pH value of plating was 2; (3) the concentration of MWCNTs and STAB in plating solution was 3 and 0.5 g/L, respectively; (4) the pulse current density was 20 A/dm^2; and (5) post-electroplating annealing was at 400 °C for 1 h. The density of these composite films was high. MWCNTs were evenly distributed, entangled with each other, and embedded into the copper grains forming interconnected mesh structure. Compared with pure Cu films prepared under the same conditions, Cu–MWCNTs composite films have significantly lower resistivity (3.19×10^{-8} Ω M), better hardness (53.5HV) and corrosion resistance. (The corrosion rate is 34.67 mm/year.) The resistivity and the corrosion rate decreased by $\sim 13\%$ and ~ 2.3 times, while the Vickers hardness increased by $\sim 23\%$.

References

1. I.S. Batra, A. Laik, G.B. Kale et al., Microstructure and Properties of a Cu-Ti-Co Alloy, *Mater. Sci. Eng.*, 2005, **402**(1–2), p 118–125
2. W.A. Monteiro, J.A.G. Carrio, C.R. Silveira et al., Structural and Electrical Properties of Copper-Nickel-Aluminum Alloys Obtained by Conventional Powder Metallurgy Method, *Mater. Sci. Forum*, 2010, **41**, p 660–661
3. S. Lijima, Helical Microtubules of Graphitic Carbon, *Nature*, 1991, **354**(6348), p 56–58
4. A. Oberlin, M. Endo, and T. Koyama, Filamentous Growth of Carbon Through Benzene Decomposition, *J. Cryst. Growth*, 1976, **32**(3), p 335–349
5. P.G. Wiles and J. Abrahamson, Carbon Fiber Layers on Arc Electrodes-I: Their Properties and Cool-Down Behavior, *Carbon*, 1978, **16**(5), p 341–349
6. J. Abrahamson, P.G. Wiles, and B.L. Rhoades, Structure of Carbon Fibers Found on Carbon Arc Anodes, *Carbon*, 1999, **37**(11), p 1873–1874
7. E.W. Wong, P.E. Sheehan, and C.M. Lieber, Nanobeam Mechanics: Elasticity, Strength, and Toughness of Nanorods and Nanotubes, *Science*, 1997, **277**(5334), p 1971–1975
8. R.S. Ruoff, D. Qian, and W.K. Liu, Mechanical Properties of Carbon Nanotubes: Theoretical Predictions and Experimental Measurements, *C. R. Phys.*, 2003, **4**(9), p 993–1008
9. S. Zhang and Q. Chen, Fabrication of MWCNT Incorporated Sn-Bi Composite, *Compos. B Eng.*, 2014, **58**, p 275–278
10. F. Wang, S. Arai, and M. Endo, The Preparation of Multi-walled Carbon Nanotubes with a Ni-P Coating by an Electroless Deposition Process, *Carbon*, 2005, **43**(8), p 1716–1721
11. X.H. Chen, C.S. Chen, H.N. Xiao et al., Dry Friction and Wear Characteristics of Nickel/Carbon Nanotube Electroless Composite Deposits, *Tribol. Int.*, 2006, **39**(1), p 22–28
12. S. Arai, A. Fujimori, M. Murai et al., Excellent Solid Lubrication of Electrodeposited Nickel-Multiwalled Carbon Nanotube Composite Films, *Mater. Lett.*, 2008, **62**(20), p 3545–3548
13. S. Arai and M. Endo, Carbon Nanofiber-Copper Composite Powder Prepared by Electrodeposition, *Electrochem. Commun.*, 2003, **5**(9), p 797–799
14. S. Arai and M. Endo, Various Carbon Nanofiber-Copper Composite Films Prepared by Electrodeposition, *Electrochem. Commun.*, 2005, **7**(1), p 19–22
15. H. Huang, C.H. Liu, Y. Wu et al., Aligned Carbon Nanotube Composite Films for Thermal Management, *Adv. Mater.*, 2005, **17**(13), p 1652–1656
16. A. Ghorbani, S. Sheibani, and A. Ataie, Microstructure and Mechanical Properties of Consolidated Cu-Cr-CNT Nanocomposite Prepared Via Powder Metallurgy, *J. Alloys Compd.*, 2018, **732**, p 818–827
17. F. Wang, S. Arai, K.C. Park, K. Takeuchi, Y.J. Kim, and M. Endo, Synthesis of Carbon Nanotube-Supported Nickel-Phosphorus Nanoparticles by an Electroless Process, *Carbon*, 2006, **44**, p 1307–1310
18. B.J.C. Thomas, M.S.P. Shaffer, S. Freeman, M. Koopman, K.K. Chawla, and A.R. Boccaccini, Electrophoretic Deposition of Carbon Nanotubes on Metallic Surfaces, *Key Eng. Mater.*, 2006, **314**, p 141–146
19. S. Arai, M. Endo, and N. Kaneko, Ni-Deposited Multi-walled Carbon Nanotubes by Electrodeposition, *Carbon*, 2004, **42**, p 641–644
20. F. Wang, S. Arai, and M. Endo, Preparation of Nickel-Carbon Nanofiber Composites by a Pulse-Reverse Electrodeposition Process, *Electrochem. Commun.*, 2005, **7**, p 674–678

21. Y. Feng and S.L. Burkett, Modeling a Copper/Carbon Nanotube Composite for Applications in Electronic Packaging, *Comput. Mater. Sci. Sci.*, 2015, **97**, p 1–6

22. P.M. Hannula, A. Peltonen, J. Aromaa et al., Carbon Nanotube-Copper Composites by Electrodeposition on Carbon Nanotube Fibers, *Carbon*, 2016, **107**, p 281–287

23. K. Jagannadham, Electrical Conductivity of Copper-Graphene Composite Films Synthesized by Electrochemical Deposition with Exfoliated Grapheme Platelets, *J. Vac. Sci. Technol. B*, 2012, **30**(3), p 03D109-1–03D109-9

24. T. Guo, P. Nikolaev, A. Thess et al., Catalytic Growth of Single-Walled Nanotubes by Laser Vaporization, *Chem. Phys. Lett.*, 1995, **243**(1), p 49–54

25. J. Laudenbach, D. Schmid, F. Herziger et al., Diameter Dependence of the Defect-Induced Raman Modes in Functionalized Carbon Nanotubes, *Carbon*, 2017, **112**, p 1–7

26. Y. Wang and Y.F. He, A Review on Adsorption of Metal Ions from Solution by Carbon Nanotubes, *New Chem. Mater.*, 2010, **38**(3), p 32–33

27. N.S. Qu, K.C. Chan, and D. Zhu, Pulse co-Electrodeposition of Nano Al₂O₃ Whiskers Nickel Composite Coating, *Scr. Mater.*, 2004, **50**(8), p 1131–1134

28. M.M. Tan, X.Y. Ye, X.H. Wang et al., Improving Contact of CNT-Metal by Annealing, *J. Funct. Mater. Devices*, 2008, **14**(1), p 227–230

29. P. Liu, D. Xu, Z. Li et al., Fabrication of CNTs/Cu Composite Thin Films for Interconnects Application, *Microelectron. Eng.*, 2008, **85**(10), p 1984–1987

30. H.C. Kim, T.L. Alford, and D.R. Allee, Thickness Dependence on the Thermal Stability of Silver Thin Films, *Appl. Phys. Lett.*, 2002, **81**(22), p 4287–4289

31. R. Manu and S. Priya, Implication of Electrodeposition Parameters on the Architecture Behavior of MWCNT-Incorporated Metal Matrix, *Appl. Surf. Sci.*, 2013, **284**(1), p 270–277